A GEOMETRIC MODEL FOR CYLINDER-CYLINDER IMPACT WITH APPLICATION TO VERTEBRAE MOTION SIMULATION

ANDRÉS KECSKEMÉTHY
Institut für Mechanik und Getriebelehre,
Technische Universität Graz
`email: kecskemethy@mechanik.tu-graz.ac.at`

CHRISTIAN LANGE
Institut für Mechanik und Getriebelehre,
Technische Universität Graz
`email: lange@mechanik.tu-graz.ac.at`

AND

GERALD GRABNER
Institut für Mechanik und Getriebelehre,
Technische Universität Graz
`email: grabner@mechanik.tu-graz.ac.at`

Abstract: The reconstruction of inter-vertebral motion of the human cervical spine, although basically understood, still poses many open problems. This is so because pairs of vertebrae undergo in general six-dimensional motion relative to one another, but display a high degree of coupling between gross translational and rotational degrees-of-freedom due to restraints imposed by ligaments and muscles and the compliant nature of the intervertebral discs (White and Panjabi, 1990). Described in this paper is the mathematical modeling of a vertebrae pair using multibody methods and impact analysis techniques with elementary contact geometry for the facet joints. The results are compared with existing approaches and with experimental data, showing a good agreement with the latter and an efficiency boost compared to existing approaches by a factor of 350. The investigations are focused on the vertebrae pair C5–C6 but can be easily extended to other vertebrae.

1. Introduction

In the reduction of medical costs, the improvement of human disease therapies, the development of new techniques for injury prevention measures,

and many other fields related to human life, biomechanics is playing an increasingly important role. Hereby, the human spine is given particular attention, due to its frequent involvement in accident-induced injuries and almost epidemic appearance in common diseases such as low back pain. In this setting, reconstruction of inter-vertebral motion, although basically understood, still poses many open problems. This is so because pairs of vertebrae undergo in general six-dimensional motion relative to one another, but display a high degree of coupling between gross translational and rotational degrees-of-freedom due to restraints imposed by ligaments and muscles and the compliant nature of the inter-vertebral discs (White and Panjabi, 1990). This paper deals with the mechanical modeling of the motion between vertebrae pair C5–C6 of the human cervical spine using notions from elementary contact mechanics. The underlying theory is developed such that it can be also applied to other vertebrae pair.

2. MADYMO Model

MADYMO is a world-wide standard for occupant safety analysis. It was chosen in the present context for creating a reference computer model of the kinematic, static and dynamic intervertebral interactions. The facet joints were specified as `Ellipsoid-Ellipsoid Contact Interactions`. The visco-elastic behavior of the intervertebral disc was implemented by connecting the origins of the vertebra body reference systems through `Point-Restraints` for the translational part and `Cardan Restraints` for the rotational part, and supplying appropriate stiffness parameters for the ensuing relative degrees of freedom. Furthermore, six ligaments of type `Kelvin Element` were attached to the vertebrae. Data for the model parameters were employed according to de Jager (1996). The determination of static equilibrium poses of the vertebrae pair requires the computation of dynamics for the movable vertebra C5 until oscillations are damped out.

3. M⬚BILE Model

As an alternative approach, an object-oriented model of the vertebrae pair was implemented using the multibody program library M⬚BILE (Kecskeméthy, 1999). For the unilateral constraints of the facet joints, a class `MoRegImpCircleCircle` representing the contact of two cylinder faces, either in edge-edge, edge-face, or face-face (flat) contact was implemented and included in the M⬚BILE library. Contact is hereby regarded as a non-smooth state transition, with appropriate state event objects "firing" when a state transition takes place. This restarts the integrator with appropriate initial conditions, making the simulation more efficient than without stop conditions. State transition from flat contact to the other two
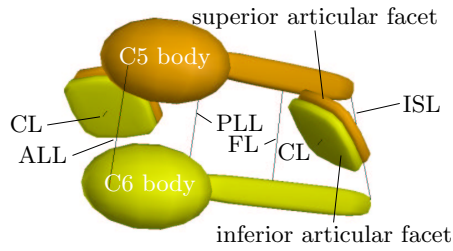
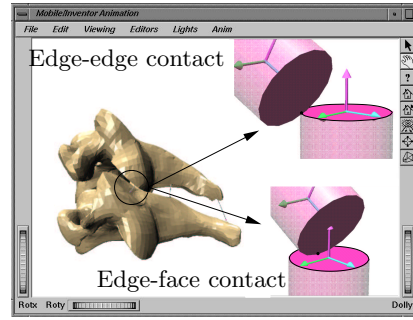*Figure 1.* C5–C6 MADYMO ellipsoid model.   *Figure 2.* C5–C6 MⓞBILE model.

types of contact and vice-versa is computed using a novel blending function, which avoids zig-zagging of state transitions for the nearby flat case. All other components, i.e., ligaments, the intervertebral disc, and stiffnesses of the facet joints, were modeled as in the MADYMO reference model. Static equilibrium poses were computed using the built-in object `MoStaticEquilibriumFinder` of MⓞBILE, which works with a Newton-Raphson algorithm. This rendered a highly efficient code that made it possible to move the vertebrae pair online in quasistatic analysis, using appropriate software sliders which change the system parameters interactively.

3.1. IMPACT ANALYSIS

In order to obtain efficient and accurate computer models, a set of impact geometry situations was investigated, regarding the facet joints as the end faces of two cylinders touching each other. This assumption seems justified due to the almost flat shape of the articulated surfaces, and proved to be sufficiently accurate in the ensuing simulations. In this setting, four possible contact situations can occur: (1) the edge of the upper cylinder touches the flat end of the lower cylinder (Fig. 2, right bottom); (2) the edge of the upper cylinder touches the egde of the lower cylinder (Fig. 2, right top); (3) the edge of the lower cylinder touches the flat end of the upper cylinder (not shown); and (4) both flat ends of the cylinders rest flatly upon each other.

For the derivation of the appropriate contact mechanics, it is necessary to discern between skew and flat contact, as explained below.

3.1.1. *Skew contact model*
Skew contact means that the angle between the faces of the colliding cylinders is finite. For this case three different contact configurations may occur: (1) contact of the edge of disc 1 on the face of disc 2 (Fig. 3); (2) contact
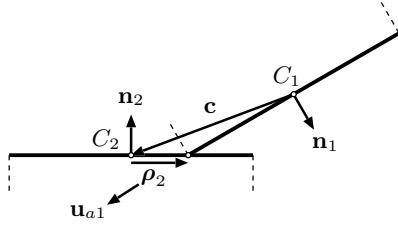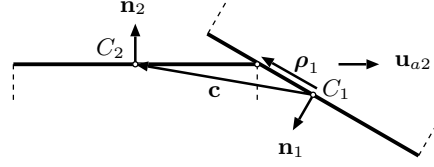
Figure 3. Contact on disc 2.   *Figure 4.* Contact on disc 1.

of the edge of disc 2 on the face of disc 1 (Fig. 4); (3) contact of the edge of disc 1 with the edge of disc 2 (Fig. 2, right top).

For case (1), the position vector $\boldsymbol{\rho}_2$ from the center C_2 of disc 2 to the contact point can be written as

$$\boldsymbol{\rho}_2 = -\mathbf{c} + r_1\,\mathbf{u}_{a1} \quad , \tag{1}$$

where $\mathbf{c} = \mathbf{c}_2 - \mathbf{c}_1$ connects the center C_1 of disc 1 with C_2, and r_1 is the radius of disc 1. $\mathbf{u}_{a1}$ denotes the unit vector perpendicular to the line of intersection l of the two disc planes π_1 and π_2 with line of action passing through C_1. Denoting the unit vectors normal to the cylinder faces 1 and 2, respectively, as $\mathbf{n}_1$ and $\mathbf{n}_2$, and setting

$$\mathbf{u} = \frac{\mathbf{n}_1 \times \mathbf{n}_2}{\|\mathbf{n}_1 \times \mathbf{n}_2\|} \quad ,$$

it follows

$$\mathbf{u}_{a1} = \mathbf{n}_1 \times \mathbf{u} \quad .$$

When contact of the edge of disc 2 on the face of disc 1 (case 2) occurs, the position vector $\boldsymbol{\rho}_1$ pointing from the center of disc 1 to the contact point becomes

$$\boldsymbol{\rho}_1 = \mathbf{c} + r_2\,\mathbf{u}_{a2} \quad , \tag{2}$$

where r_2 is the radius of disc 2 and $\mathbf{u}_{a2}$ is the unit vector perpendicular to the common line of intersection with line of action passing through C_2,

$$\mathbf{u}_{a2} = -\mathbf{n}_2 \times \mathbf{u} \quad .$$

Contact takes place whenever $\|\boldsymbol{\rho}_1\| < r_1$ (case 1) or $\|\boldsymbol{\rho}_2\| < r_2$ (case 2). In order to simulate impact using a regularized approach, the neighborhood of

the contact point is regarded as compliant. The corresponding penetration d is defined as acting normal to the face of the cylinder onto which the edge of the other rests. One hence obtains

$$d = \begin{cases} \mathbf{c} \cdot \mathbf{n}_1 - r_2 \sin\alpha & : & \text{case } 1 \\ -\mathbf{c} \cdot \mathbf{n}_2 - r_1 \sin\alpha & : & \text{case } 2 \end{cases} \quad .$$

The resulting contact force is normal to this face with magnitude equal to a user-defined stiffness coefficient multiplied by the penetration d, i.e., a virtual linear spring element is attached between the edge of the one cylinder and the face of the other at the contact point with line of action normal to the cylinder face described above.
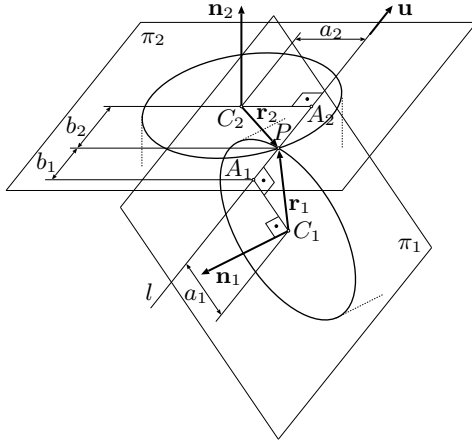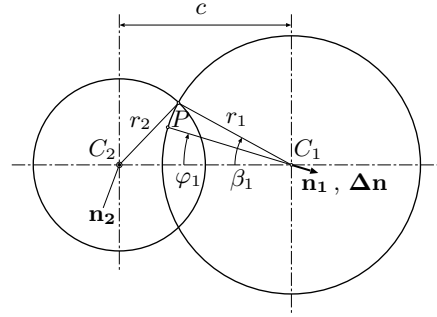

Figure 5. Frictionless circle-circle contact.

Figure 6. Projection onto contact plane for flat contact.

For edge-edge contact (case 3) analysis, first, the distances a_1 and a_2 from the center points of the two circles to the common line of intersection of the disc planes are established. It holds (Fig. 5):

$$a_1 = \frac{(\mathbf{c}_2 - \mathbf{c}_1) \cdot \mathbf{n}_2}{\mathbf{u}_{a1} \cdot \mathbf{n}_2} = \frac{\mathbf{c} \cdot \mathbf{n}_2}{\mathbf{u}_{a1} \cdot \mathbf{n}_2} \ , \quad a_2 = \frac{(\mathbf{c}_1 - \mathbf{c}_2) \cdot \mathbf{n}_1}{\mathbf{u}_{a2} \cdot \mathbf{n}_1} = -\frac{\mathbf{c} \cdot \mathbf{n}_1}{\mathbf{u}_{a2} \cdot \mathbf{n}_1} \ .$$

With these, the distances b_1 and b_2 from the feet of the circle midpoints at the common line of intersection of the disc planes to the contact point P can be computed as

$$b_{1,2} = \sqrt{r_{1,2}{}^2 - a_{1,2}{}^2} \quad .$$

Note that b_1 and b_2 are real whenever the common line of intersection of the disc planes intersects both circles.

Penetration d is defined in this case as acting along the common line of intersection of the disc planes. It follows

$$d = |\mathbf{c} \cdot \mathbf{u}| - (b_1 + b_2).$$

At contact, $d = 0$, and hence the contact condition becomes

$$b_1 + b_2 = |\mathbf{c} \cdot \mathbf{u}|.$$

3.1.2. *Flat contact model*

In the case of an almost flat contact between the cylinder surfaces, the formulas derived above become singular. In this case, one can establish the contact geometry by projecting the circles on the plane normal to the (almost parallel) cylinder axes.

In the following, the case of contact between the edge of circle 1 and the flat end surface of cylinder 2 is regarded (Fig. 6). The case of contact between circle 2 and the end surface of cylinder 1 is treated analogously. Let P be the contact point and assume that the projection plane is taken as π_2. The inclination of cylinder 1 with respect to cylinder 2 is assumed to be so small that the distortion of circle 1 to an ellipse is negligible. Contact is maintained whenever the angle φ_1, subtended by the interconnection line of the two circle centers and the ray passing through C_1 and the contact point, is less than or equal to the angle β_1, subtended by $\overline{C_1\,C_2}$ and the ray passing through C_1 and the intersection point of both circles.

For the angle β_1, one readily obtains

$$\cos \beta_1 = \frac{1}{2\,r_1\,c}\left(r_1^2 - r_2^2 + c^2\right),$$

where $c = \overline{C_1\,C_2}$. The angle φ_1 can be calculated as

$$\cos \varphi_1 = \frac{-\mathbf{c} \cdot \mathbf{\Delta n}}{|\mathbf{c}|\,|\mathbf{\Delta n}|},$$

with $\mathbf{\Delta n} = \mathbf{n}_1 + \mathbf{n}_2$, a quantity that would correspond to the "difference" of the circle normals when both were oriented towards the same half-space.

By inserting the above expressions in the contact condition $\cos \varphi_1 \geq \cos \beta_1$, one obtains as condition for a contact of the edge of circle 1 on the end surface of cylinder 2, or similarly for a contact of the edge of circle 2 on the end surface of cylinder 1, respectively

$$-\mathbf{c} \cdot \mathbf{\Delta n} \geq \frac{1}{2}\frac{|\mathbf{\Delta n}|}{r_1}\left(r_1^2 - r_2^2 + c^2\right) \quad \text{or,} \quad \mathbf{c} \cdot \mathbf{\Delta n} \geq \frac{1}{2}\frac{|\mathbf{\Delta n}|}{r_2}\left(r_2^2 - r_1^2 + c^2\right).$$

By regarding the expression for $\cos \beta_1$ above, the following case distinctions can be made:

$$\frac{1}{2\, r_1\, c}(r_1^2 - r_2^2 + c^2) \quad \begin{cases} > 1 & : \quad \text{(virtual) contact outside of disc 2} \\ < -1 & : \quad \text{disc 1 fully contained in disc 2} \\ \text{else} & : \quad \text{partial overlapping of discs 1 and 2} \end{cases} ,$$

By the same token, after establishing a similar expression for $\cos \beta_2$, one obtains the case distinctions

$$\frac{1}{2\, r_2\, c}(r_2^2 - r_1^2 + c^2) \quad \begin{cases} > 1 & : \quad \text{(virtual) contact outside of circle 1} \\ < -1 & : \quad \text{disc 2 fully contained in disc 1} \\ \text{else} & : \quad \text{partial overlapping of discs 2 and 1} \end{cases} .$$

The above derived formulas fail to be applicable when the circles are fully parallel because in this case the vector $\boldsymbol{\Delta n}$ vanishes. For this case, one can assume the contact to take place at the center point M of the segment of the center interconnection line contained in the common contact patch (for partially overlapping discs). The distance between C_1 and M is given by

$$L = c - r_2 + \frac{r_1 + r_2 - c}{2} = \frac{c + r_1 - r_2}{2} \ .$$

If disc 1 lies completely within disc 2, one can assume that the contact point M coincides with C_1. Correspondingly, one can define the contact point M as incident with C_2 when disc 2 lies completely within disc 1.

3.1.3. *State transition*

For smooth transition between the fully parallel case and the almost parallel case, a novel procedure is proposed, where a virtual contact point is obtained by interconnecting M and P and employing a blending function to position the virtual contact point between these two extremes as a function of the angle between the circle normals. The blending function chosen in the present context is

$$r = r_0\, (1 - e^{-C\, \sin \alpha}),$$

with r_0 being the distance between M and P, C a constant and α the subtended angle by the circle normals.

The basic idea of the blending function is illustrated in Fig. 8 for the case of a contact of a cylinder with a plane. The virtual contact point P' lies between the center of the cylinder and its circumference along the line of intersection of the plane subtended by the surface normals $\mathbf{n}_p$ and $\mathbf{n}_c$
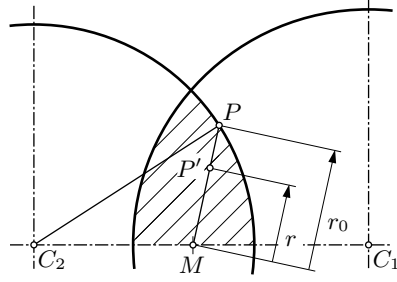
Figure 7. Blending ray within contact patch for flat cylinder-cylinder contact.
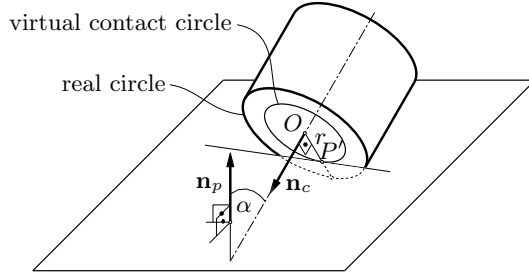

Figure 8. Disc-plane contact.

with the cylinder end surface through the center of the circle. A particular property of the blending function described above is that it renders a stabilizing moment in direction perpendicular to both surface normals that makes fully stable flat contact possible. Hence, no further computations and state transition tracking procedures are necessary for transition from steep to flat contact as well as for transition from one edge to the other. A result of a simulation of the contact between a disc and a plane is displayed in Fig. 9, where the relative indentation r/r_0 (with r_0 being the original disc radius and r the actual distance to the circle center) and the sine of the inclination angle α are plotted over time. Clearly, the motion asymptotically approaches fully flat contact with the virtual contact point at the circle center.
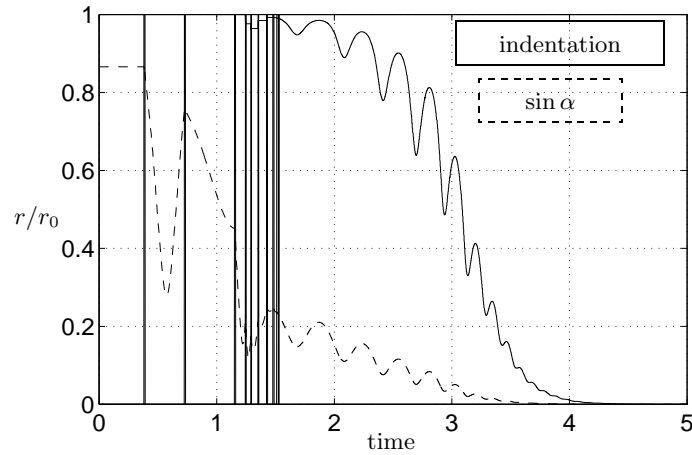

Figure 9. Example of smooth steep-to-flat transition.

4. Model Validation

Both vertebrae pair models developed with the MADYMO package and the MⒷBILE library were compared and validated with the experimental results reported by Moroney (1998) and the computer simulation performed by de Jager (1996). The simulations compute the translational and rotational deflections from the reference position of vertebra C5 to the new state of equilibrium for nine loading conditions corresponding to application of a single force (20 N) or moment (1.8 Nm) in direction of each elementary motion of C5. In this setting, the numerical values shown in Fig. 10 were obtained. Hereby, the following test loads were computed: an-
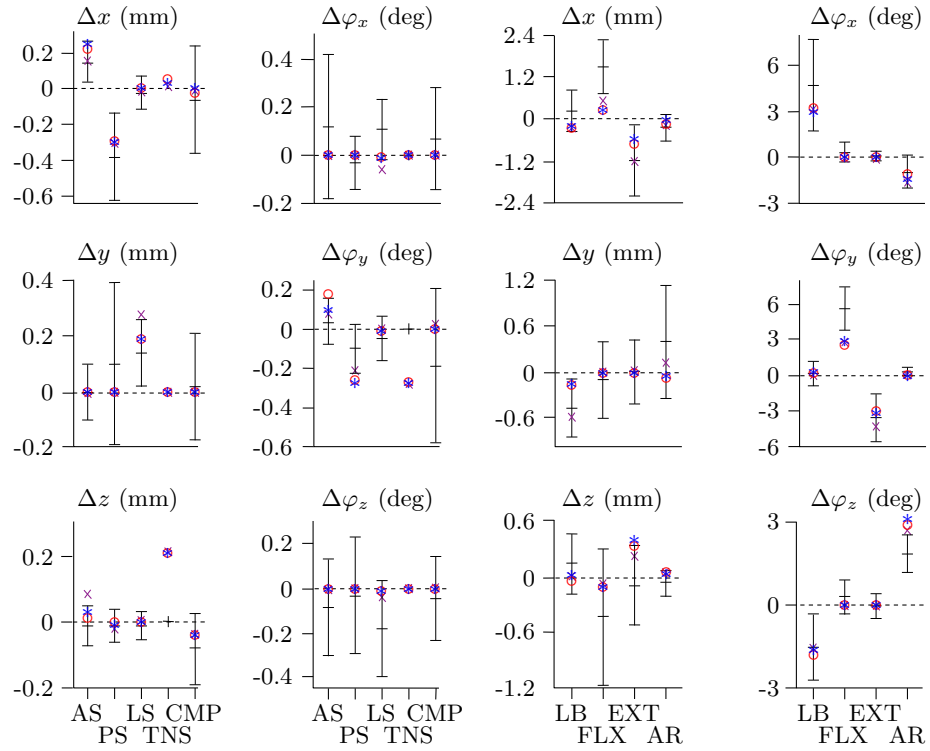

Figure 10. Model comparison of main and coupled displacements: MⒷBILE: ○, MADYMO: *, de Jager (1996): × with experimental results of Moroney (1998): + (average± SD).

terior shear (AS), posterior shear (PS) for x-translation, lateral shear (LS) for y-translation, tension (TNS) and compression (CMP) for z-translation, lateral bending (LB) for x-rotation, flexion (FLX) and extension (EXT) for

y-rotation, and axial rotation (AR) for z-rotation. As it can be seen, a good agreement between the experimental data and the computer models could be achieved. In particular, the simplified MⓄBILE model renders results that are not more inaccurate than the complex MADYMO model. However, the MⓄBILE model runs faster than the MADYMO model by a factor of 350. This allows one to compute the motion of a vertebrae pair in real-time simulation environments, in contrast to the MADYMO model, which can be used only in offline applications.

5. Conclusions

The developed impact model for vertebrae contact is suitable for efficient biofidelic prediction of intervertebral motion. It is planned to use this model for the controller of a small-scale parallel manipulator for the physical simulation of intervertebral motion, which is being currently designed.

6. Acknowledgments

References

de Jager, M., (1996), *Mathematical Head-Neck Models for Acceleration Impacts.* PhD thesis, Technische Universiteit Eindhoven.

Kecskeméthy, A., (1999), MⓄBILE 1.3 *User's Guide.* Institut für Mechanik und Getriebelehre, Technische Universität Graz.

Moroney, S. P., Schultz, A. B., Miller, J. A. A., and Anderson, G. B. J., (1988), Load-displacement properties of lower cervical spine motion segments. *Journal of Biomechanics*, vol. 21, pp. 769–779.

White, A. and Panjabi, M. M., (1990), *Clinical Biomechanics of the Spine.* J. B. Lippincott, second ed.